UC34C
LBL-22060
Preprint c.1

Lawrence Berkeley Laboratory
UNIVERSITY OF CALIFORNIA

RECEIVED
LAWRENCE
BERKELEY LABORATORY

NOV 18 1986

LIBRARY AND
DOCUMENTS SECTION

Submitted to Physical Review C

PAIR TRANSFER AT HIGH ANGULAR MOMENTA

J.L. Egido and J.O. Rasmussen

September 1986

For Reference

Not to be taken from this room

NUCLEAR SCIENCE DIVISION

LBL-22060 c.1

Prepared for the U.S. Department of Energy under Contract DE-AC03-76SF00098

DISCLAIMER

This document was prepared as an account of work sponsored by the United States Government. While this document is believed to contain correct information, neither the United States Government nor any agency thereof, nor the Regents of the University of California, nor any of their employees, makes any warranty, express or implied, or assumes any legal responsibility for the accuracy, completeness, or usefulness of any information, apparatus, product, or process disclosed, or represents that its use would not infringe privately owned rights. Reference herein to any specific commercial product, process, or service by its trade name, trademark, manufacturer, or otherwise, does not necessarily constitute or imply its endorsement, recommendation, or favoring by the United States Government or any agency thereof, or the Regents of the University of California. The views and opinions of authors expressed herein do not necessarily state or reflect those of the United States Government or any agency thereof or the Regents of the University of California.

Pair Transfer at High Angular Momenta†

J.L. Egido* and J.O. Rasmussen

Nuclear Science Division
University of California
Lawrence Berkeley Laboratory
Berkeley, CA 94720

Abstract

Realistic calculations of the pair transfer strength functions were performed for the nuclei ^{162}Dy and ^{164}Dy as a function of the angular momentum and excitation energy in the frame of the self-consistent, cranked HFB and RPA theories. At low angular momenta most of the strength is concentrated in the ground-to-ground transition, whereas at high angular momenta, after the pairing correlation has dropped, the strength is spread among several states located a few (≤4) MeV above the Yrast line.

Introduction

In recent years high-spin physics has provided a large share of the new and interesting problems in low-energy nuclear physics. The monotony in the rotational moments-of-inertia was broken by the backbending phenomenon[1]; afterward, a large variety of experimental findings emerged: superdeformed nuclei,[2] terminating bands,[3,4] giant resonances built on rotational excited states,[5] and damping of rotational states,[6] to mention a few.

---

† This work was supported in part by a Fulbright/MEC grant and in part by the Director, Office of Energy Research, Division of Nuclear Physics of the Office of High Energy and Nuclear Physics of the U.S. Department of Energy under Contract DE-AC03-76SF00098.

* Permanent address: Departmento de Fisica Teorica, Universidad Autonoma de Madrid, 28049 Madrid, Spain.

Many of the above-mentioned findings were unexpected. A theoretical prediction long sought is the Mottelson-Valatin effect,[7] which says that a deformed nucleus which is superfluid in the ground state (I=0) will experience a phase transition to a normal phase at high angular momentum due to the Coriolis field, which breaks the Cooper pairs. Since that notable 1960 prediction, several new observations have been hailed as the pairing collapse, but there has been no definitive proof. Proof is difficult, in part, because there is a gapless superconductivity at high spins that makes it very hard to observe spectral features directly related to the pairing. Theoretical studies, or interpretations,[8,9] are in seeming disagreement. Mean-field theories do predict a sharp collapse of the pairing gap (at spins from 10ħ to 20ħ for rare earths), whereas projected theories find just a smooth weakening of the pairing correlations up to very high spins. The projected theories take into account many more correlations, and should therefore be more reliable. There exists, however, some arbitrariness in the definition of the pairing gap.

It has long been suggested that more direct evidence about pairing correlations could be found by looking at pair transfer strengths, rather than at energy level patterns. Recently, there has been some work in this direction,[10,11,12,17] in particular, Guidry et al. developed classical orbital methods to estimate how well heavy ion transfer reactions could be used to study pair transfer at the higher rotational levels Coulomb-excited on the inward path of the projectile. While sufficiently heavy ions have not yet been used in such studies to probe the interesting backbending region, recent Oak Ridge work with Ni and Sn projectiles has already illuminated features of one- and two-neutron transfer at higher spins. In particular the reactions seem predominantly to be "cold transfer," going to states fairly close to the Yrast line.

Theoretical studies of pair transfer matrix elements at high angular momenta have been scarce and limited to simplified model calculations.[9] The purpose of this paper is to carry out more realistic calculations of the pair transfer matrix elements as a function of the angular momentum for the recently-measured[12] nuclei ^{162}Dy and ^{164}Dy. We hope that this work may shed some light on the process and on the understanding of the experimental situation. The calculations were done in the frame of the self-consistent cranked Hartree-Fock-Bogoliubov theory (CHFB), using the hamiltonian and configuration space of Baranger and Kumar.[13] To take into account transfer to collective pairing vibrations we also calculated the transfer with Random-Phase-Approximation wave functions based on the self-consistent field (CRPA).

II. Theory

The general theory of pair transfer in non-rotational nuclei can be found in work of Bohr and Mottelson,[14] but since there is not a "standard" description of the pair-transfer amplitude for the case of deformed rotating nuclei, we shall introduce some notation and justify our approximations.

II.1 The amplitudes for pair transfer

The situation we try to describe is illustrated in Fig. 1. In a pair transfer reaction a Cooper pair is deposited (removed) from the rotating nucleus (A, E_{Yrast}, I) leading to the nucleus (A ± 2, I) at the Yrast level or at an excited state. One could also have pair transfer involving transfer of angular momentum; this would correspond to a transition mediated by higher multipolarities, and such will not be considered in this paper. We shall in what follows refer specifically to neutron transfer, but obviously all the formulas apply equally well for proton transfer by merely replacing N by Z.

Let $\{c_k^+, c_k\}$ be a complete set of single particle operators characterized by the quantum numbers $k \equiv (\tau, n, l, j, m)$. the operator

$$P^+ = \frac{1}{2} \sum_k c_k^+ c_{\bar{k}}^+ \tag{1}$$

creates a Cooper pair for protons ($\tau \equiv p$) or neutrons ($\tau \equiv n$). Let now $|\Psi_o(I)\rangle_N$ and $|\Psi_o(I)\rangle_{N+2}$ represent the Yrast states at angular momentum I for the nucleus (N,Z) and (N+2,Z) respectively, and $|\Psi_f(I)\rangle_{N+2}$ an excited state of the (N+2,Z) nucleus. We shall omit the indices Z, from now on, to simplify the notation.

The the ground-to-ground transfer at angular momentum I is given by

$$S_I(g, N \to N+2) = |{}_{N+2}\langle\Psi_o(I)\ |P^+|\Psi_o(I)\rangle_N|^2 \tag{2}$$

and that to an excited state f given by

$$S_I(f,\ N \to N+2) = |{}_{N+2}\langle\Psi_f(I)|P^+\ |\Psi_o(I)\rangle_N|^2 \tag{3}$$

A similar definition to expressions (2) and (3) has been given by Kumar[15] for I=0 and deformed nuclei. The amplitudes for the removal of a Cooper pair are given by using the operator P instead of P^+ and using the wave functions corresponding to a nucleus with N-2 particles.

II.2 The wave functions

The next important task is to specify the approximations we use for the states $|\Psi_o(I)\rangle_N$ and $|\Psi_f(I)\rangle_{N+2}$. In dealing with high-spin states one has to consider sufficiently general wave functions to include collective as well as single particle degree of freedom which will allow for changes in the shape,

the pairing potential and the single-particle alignments. A theory that includes such features and that has explained most of the high-spin phenomena is the HFB approximation combined with the cranking procedure, also known as self-consistent cranking.[16] We shall denote the mean field approximation to $|\Psi_0(I)\rangle$ of eqs. (2) and (3) by $|\phi\rangle$. One might be tempted to make a better approximation by particle number projection combined eventually with some kind of generator coordinate method to describe properly the collective states. Such types of calculations could be done[17] for the ground-to-ground transfer where only a single final state is involved, but for the thousands of excited states of eq. (3) in which we are mainly interested, it is numerically not feasible.

In the cranked HFB approximation the expectation value of the operator

$$\hat{H}' = \hat{H} - \omega\hat{J}_x - \lambda\hat{N} \tag{4}$$

is minimized in the space of generalized Slater determinants $|\phi\rangle$, under the constraint of correct average angular momentum and particle number, i.e. the cranking velocity ω and the chemical potential λ are adjusted to fulfill the given constraints.

The variational problem which one faces is

$$\frac{\langle\phi|\hat{H}'|\phi\rangle}{\partial\phi} = 0 \tag{5}$$

with

$$\begin{aligned} \langle\phi|\hat{J}_x|\phi\rangle &= \sqrt{I\,(I+1)} \\ \langle\phi|\hat{N}|\phi\rangle &= N \end{aligned} \tag{6}$$

Now, to calculate the amplitudes (2)-(3) in the mean field approximation one should, at least in principle, solve the equations (5-6) for the system

with N neutrons to obtain $|\phi\rangle_N$ and for N+2 neutrons for $|\phi\rangle_{N+2}$. Solving the equations is not so bad compared with the formidable task of trying to evaluate the overlaps in eq. (3) for the thousands of excited states which already appear at a few MeV of excitation energy in realistic calculations.

Fortunately, in most of the cases it is not necessary to work with two different bases $|N\rangle$ and $|N\pm2\rangle$ for the following reasons: At low spins, where the pairing correlations are sufficiently strong, the nucleus behaves to a large extent as a Cooper pair condensate, so that in going from N to N+2 one does not expect drastic changes in the wave functions. At the very high spin limit $I \gg 1$ in the mean-field approximation the gap goes to zero and one gets eigenstates of the particle number. Therefore the states of the nucleus with N+2 (N-2) particles can be described approximately as the two particle (hole) states of the nucleus with N particles. In the region of medium spins and high excitation energy we need not be concerned because these states are pure holes or pure particles and we again have good particle number for such excitation. The questionable region is for medium spins and for states near the Yrast band. Nevertheless, we shall describe the states of the N±2 particle nuclides in terms of the N particle nuclide, recognizing the limitations of this approach.

Summarizing the discussion above, we make the following approximations:

(a) For the ground-to-ground transfer at angular momentum I

$$S_I(g,N \to N+2) = |{}_{N+2}\langle\phi|P^+|\phi\rangle_N|^2 \approx |\langle\phi|P^+|\phi\rangle|^2 = \left(\frac{\Delta}{G}\right)^2 \qquad (7)$$

In the last part we have used the definition of the gap parameter Δ, and introduced the pairing strength G.

(b) For the ground-to-excited state transfer in CHFB theory

$$S_I(f,\ N \to N+2\rangle = |{}_{N+2}\langle\phi_f|P^+|\phi\rangle_N|^2 \approx |\langle\phi|\alpha_k\alpha_\ell P^+|\phi\rangle|^2 \tag{8}$$

The operators a_k define the vacuum $|\phi\rangle$, i.e.,

$$\alpha_k|\phi\rangle = 0,\ \forall k$$

they are related to the operators c_m of eq. (1) by the Bogoliubov transformation

$$\alpha_k^+ = \sum_m U_{mk}\ c_m^+ + V_{mk}c_m$$

The excitation energy of the state f is given by $E_f = E_k + E_l$, where E_k, E_l are quasiparticle energies. In (7) and (8) the wave function $|\phi\rangle$ satisfies the conditions (6).

Another advantage of the CHFB approximation is that it allows, relatively easy, to incorporate further correlations in the wave functions as to describe collective vibrations around the mean field values. This approximation, the CRPA, has been used to describe the β and γ collective vibrations at high spin, and good agreement with experiment was found.[18] In this paper we use the same approach to calculate the collective pair transfer. Expression (7) for the ground-ground transfer remains unaltered, but expression (8) becomes for the ground-excited transfer in CRPA

(c) $$S_I(f,N \to N+2) \approx |\langle\Psi|B_\rho P^+|\Psi\rangle|^2\ , \tag{9}$$

where now $|\Psi\rangle$ is the vacuum for the one-boson states B_ρ, which are solutions of the CRPA equations built on the minimum described by $|\phi\rangle$. Energy $E_f \equiv \Omega_\rho$ is the excitation energy of B_ρ^+.

We shall refer to (8) as the uncorrelated transfer and to (9) as the correlated transfer. Aside from the feature that one can describe collective phenomena in the CRPA, another important point is that in this approximation the Goldstone modes associated with the broken symmetries in the CHFB approximation separate exactly from the normal modes and go to zero energy.

II.3 Hamiltonian and configuration space

For a realistic evaluation of the pair transfer amplitudes in the CHFB and CRPA theories we shall use the hamiltonian and configuration space of Kumar-Baranger,[13] which has been used with considerable success by several authors for the description of high-spin states. The ingredients of the hamiltonian are the pairing-plus-quadrupole effective interactions. In a compact notation

$$H = \varepsilon + \tfrac{1}{2} \sum_\rho \chi_\rho D_\rho^+ \cdot D_\rho \ , \tag{10}$$

where ε are the spherical single-particle energies and the hermitian (or antihermitian) operator D_ρ, runs over the five quadrupole operators Q_μ, symmetrized with respect to the Goodman Symmetry,[19] and $P^+ \pm P$. The operator P^+ defined in (1) creates proton (or neutron) Cooper pairs. The configuration space contains the spherical oscillator shells with the principal quantum numbers N=4,5 for protons and N=5 and 6 for neutrons. The force constants χ_Q, and χ_P ($\equiv G_P$ or G_N) were adjusted to the ground state properties of the rare-earth nuclei. Further details can be found in ref. 13.

One of the more attractive features of the hamiltonian (10) is the separability of the forces, which allows drastic simplifications in solving the CHFB equations (5)-(6). In the RPA case it reduces the diagonalization of a huge matrix to the simple problem of finding the zeroes of a determinant of dimensionality equal to the number of terms in expression (10). For the calculation of the transfer amplitudes, eq. (9), in the CRPA, the separability allows one to evaluate those qualities without solving the RPA equations.

For any hermitian (antihermitian operator) one-body operator $\hat{F}$, the strength function at energy E is given by[20]

$$S(E) = \sum_f |\langle f|\hat{F}|i\rangle|^2 \delta(E - (E_f - E_i)) = -\frac{1}{\pi} \operatorname{Im} R_{FF}(E) \tag{11}$$

where R(E) is the response function at energy E

$$R(E) = \frac{R^o(E)}{1-\chi R^o(E)} \tag{12}$$

and $R^o(E)$ the free response function, with matrix elements

$$R^o_{AB}(E) = \tfrac{1}{2} \sum_{k\ell} \left(\frac{A^{20*}_{k\ell} B^{20}_{k\ell}}{E - E_k - E_\ell + i\eta} - \frac{A^{02*}_{k\ell} \cdot B^{02*}_{k\ell}}{E + E_k + E_\ell + i\eta} \right) \tag{13}$$

$A^{20}_{k\ell}$ and $A^{02}_{k\ell}$ being the 20 and 02 parts of the representation of the operator $\hat{A}$ in the basis determined by the CHFB solution and E_k, the corresponding quasi-particles energies. The operators A and B run over the D_ρ operators of eq. (10) and determine the dimension of the matrix R. This means[20] that in the case of the CRPA, when $|f\rangle$ are one boson states, one can obtain the correlated

strength function just by representing the corresponding operators in the CHFB basis and making the matrix inversion of eq. (12).

The use of the linear response theory (LRT) formulas is specially suitable for those cases where the level density is high and it is very computationally time-consuming to find the main contributions to the strength function (11) state by state. By setting a finite value η and doing calculations with a stepsize $\Delta E \ll \eta$ one is able to reproduce the main features of the strength function. The same advantage can be used for the CHFB case just by taking R^o instead of R in expression (11).

III. Results

We apply the described formalism to the nucleus ^{162}Dy, for which recent experiments on pair transfer were done.[12] Since this nucleus turned out to have unexpectedly longlasting pairing correlations, we also studied the neighboring isotope ^{164}Dy to investigate the effect of the pairing collapse on the transfer strength at somewhat lower angular momenta.

Since the microscopic structure plays a major role, we shall first discuss some properties of the underlying mean-field. In Figure 2a we show, in the upper part, the cranking velocity, l.h.s. scale, as a function of the angular momentum for ^{162}Dy. We observe a strong backbending at approximately $I = 16\hbar$ and some alignment at $I \sim 26\hbar$. The gaps parameters, referred to the r.h.s. scale, are also shown in the same Figure. The neutron-gap decreases steadily until $I = 30\hbar$, to 260 KeV, and then suddenly drops to zero. The proton gap shows a kink at the I-value where the backbending occurs, due to the fact that at this point the cranking velocity is smaller than in the former I-value. For neutrons this effect does not show up because, as we will see, their wavefunction changes around this point. In the lower part of the

Figure we show the amount of alignment for protons and neutrons. This quantity is defined for each type of nucleon as the difference between the calculated contribution to the expectation value of J_x and the one obtained using a cubic extrapolation of the corresponding value at I = 2ħ and 4ħ, namely,

$$\langle J_x \rangle_{al} = \langle J_x \rangle - \langle J_x \rangle_{g.s.}, \tag{14}$$

where

$$\langle J_x \rangle_{g.s} = {}_0 \cdot \omega + {}_1 \cdot \omega \ . \tag{15}$$

The parameters ${}_0$ and ${}_1$ are adjusted separately for protons and neutrons. We also show the increment of alignment between the spin I and I-2.

$$\Delta \langle J_x \rangle_{al} = \langle J_x \rangle_{al_I} - \langle J_x \rangle_{al_{I-2}} \ . \tag{16}$$

This quantity peaks whenever a nucleon pair aligns, and the height of the peak indicates how fast the alignment happens. The values of $\langle J_x \rangle_{al}$ refer to the left scale, and those of $\Delta \langle J_x \rangle_{al}$ to the right one. We see now very clearly that the cause of the backbending is the alignment of a neutron pair and that the cause for the collapse of the neutron-gap at I ~ 30ħ is the alignment (small) of a second pair. The proton alignment sets in around I = 20ħ and extends until I = 30ħ, causing the decrease of the proton gap as well as the change in the slope of the cranking velocity.

In Figure 2b we show the corresponding quantities for the nucleus ^{164}Dy, seen here in a very clear example of the oscillatory character of the backbending phenomenon. The effect of adding two neutrons enhances the deformation and decreases the values of the gap parameters at I=0; both effects contribute at high spin to make the gap go to zero much faster than in the nucleus ^{162}Dy. One still can observe on the cranking velocity the effect

of the proton alignment which, as can be seen from the lower part of the Figure, behaves very similarly to ^{162}Dy. On the other hand, the backbending is smoothed out and only a small peak can be found for the neutron alignment in the lower part of the Figure. Thus, these nuclei provide two examples with different characteristics for which we shall investigate the transfer strength properties.

In Figures 3 through 7 we show the pair transfer strength as a function of the excitation energy for different values of the angular momentum. Each small Figure corresponds to a cut perpendicular to the x-axis in Figure 1 for a given value of the angular momentum. One possibility for choosing the energy origin in these graphs would be to measure the excitation energy with respect to the Yrast line of the final nucleus N+2 (N-2). In our approximation, as long as $\Delta \neq 0$, the Yrast state for the N+2 and N-2 is $|\phi\rangle_N$, but when $\Delta = 0$ the Yrast state for the N+2 (N-2) nucleus is the lowest two-particle (hole) state of $|\phi\rangle_N$. This produces a small overall shift in the strengths when $\Delta \to 0$. This shift would not be present if we had self-consistently calculated the states of the nucleus N+2 (N-2). In this case one would expect some rearrangement around $\Delta = 0$ in the states near the Fermi surface but not an overall shift in the strength. To avoid this unphysical shift around $\Delta = 0$, we refer to the origin of the excitation energies in these Figures for all I to the Yrast line of $|\phi\rangle_N$. This means that the dips in the energy region below the first peak should be ignored. We present the two above-mentioned approximations: a) The HFB approximation, i.e., we plot the quantity S(E) of formula (11), but we use the free response function R^0 of (13); and b) the RPA, where we plot S(E) but now using the correlated response function of eq. (12). In both we have used an η ($\eta = \Gamma/2$) corresponding to Γ = 0.075 MeV. The choice of this value was made by taking it as small as

possible consistent with numerical feasibility. We check in concrete examples the approximation of working with a finite η and found no loss of information. By using linear response theory in the RPA approximation, one has to be aware of a spurious nonzero contribution to the strength function of the Goldstone modes, if any. This is due to the fact that by using a finite η we give to <u>each</u> RPA-mode a Lorentzian shape of width Γ_{FWHM}. Since the Goldstone modes are not normalizable, they could in principle contribute to the strength functions, but we believe these contributions are quite small here. We avoid these contributions by working in the first two MeV with an effective pairing operator $\tilde{P}$ orthogonal to the number operator, instead of P. Lastly, to have a direct comparison between the ground-to-ground and the ground-excited-state transfer we have smeared out the ground-to-ground transfer (7), with the same width Γ as used in the LRT, between the other modes.

In Figure 3A, we show the transfer strength for neutron-pair transfer for the nucleus ^{164}Dy in the HFB approximation. The dotted line at 0.1, used to guide the eye, corresponds approximately to the single particle strength. For I = 0 the quantum number K is conserved and there is high degeneracy. This is also the cause of the large intervals without strength. The minimal values of ~0.001 are due to contributions of other modes. The transfer to excited states is of the order of magnitude of 0.1 and the ground-to-ground transfer two orders of magnitude larger. For I = 4, 8 and 12ħ, we see the effect of the Coriolis force on the strength function; the time-reversed symmetry is broken, and consequently the peaks split, and some strength appears in different places. We also observe some strength growing near the ground state. At I = 0ħ the lowest excited state transfer appears around 2 MeV, while at I = 12ħ it is about 1 MeV. The second column, I = 16, 20, 24 and 28ħ, corresponds to a regime characterized mainly by the quenching of the

ground-to-ground transfer and by a further establishment of the high spin regime: first, the holes in the spectrum are getting smaller. In particular, the one at ~5 MeV by I = 16ħ is filled by I = 28ħ; second, the concentration of strength everywhere in the spectrum and in particular the minimum values are higher than before; and third, a kind of new shell structure emerges, probably due to the band crossing, in this example at I = 16ħ, which brings about the new broad dip at about 2.5 MeV excitation energy. The third column, I = 32, 36, 40 and 44ħ, shows how the strength redistributes at the very high spin limit. In particular for I = 40 and 44h, we observe two bumps, one which extends from 1.5 to 6 MeV, centered at 3 MeV, and the other from 6 to 10 MeV centered around 7.5 MeV.

In the HFB approximation no collectivity is allowed in the wavefunction; therefore, the transfer to excited states could be changed, if some collectivity is present, in the RPA approximation. This is displayed in Figure 3B. In the first column for I = 0, we observe at first sight a similar spectrum to the HFB one. In particular, we note similarity in the spacing of the peaks. A more careful look shows that some of the peaks, like that around 4.5 MeV, split into two components which repel each other. Others, such as those around 2 MeV in the HFB spectrum, combine to produce a collective state of a strength about 10 times the single-particle estimate. At higher angular momenta, as in the HFB approximation, we see the Coriolis effects on the transfer strength. It is important to note in going from I = 0 to I = 12ħ that whereas the collectivity of the ground-to-ground transfer decreases, the collectivity of the strength for ground-low-lying excited states, although split into several components, increases. The upper part of the spectrum shows, as expected, a great similarity with the HFB one, in particular above ~4 MeV. In the second column, the collectivity of several states concentrates

to a large extent in the lowest excited state. At I = 20ħ, the strength of this peak reaches its maximum value. By I = 24 and 28ħ the first peak has moved to slightly higher energies, and the total strength to the excited states below 2.5 MeV has increased appreciably.

Since the ground-to-ground strength has dropped from the sizable value of I = 16ħ to exactly zero to I = 28 and since the strength above 3 MeV does not change very much between these two I-values, we conclude that the accumulation of strength between 0 and 2.5 MeV is probably due to the weakening of the pairing correlations in the nucleus. In the third column we perceive the shifting of the strength to higher excitation energies as a function of the angular momentum. In particular for the highest values (I = 40 and 44ħ) we observe that the strength distribution looks very spread, concentrated below 4 MeV and does not show any structure.

Figure 4 displays the transfer strength for neutron-pair removal (in part A the HFB approximation, in Part B the RPA). Since this Figure has many common features with the previous one, we shall now just comment on the differences between them. In Figure 4A, at I = 0 we have, as before, a high degree of degeneracy. The spacings in between are now smaller, and thus when we go to angular momentum 12ħ we found that the strength is more uniformly distributed. In the second column we now find that the valley that developed before at around 3 MeV now is broader and appears at about 2 MeV. In the third column we see that there is a peak at ~ 0.5 MeV of considerable strength. With respect to the RPA (Figure 4B) we find that, for all spin values, it shows more collectivity than in the pair addition case. In particular, one can see in the first column a bump about 2.5 MeV. In the second column, where the pairing correlations quenching takes place, we find again a shifting of strength from the ground-to-ground to the ground-excited

state transfer. In the very high spin limit we find most of the strength under 4 MeV, very dispersed and not showing any given structure.

In Figures 5 and 6 we show the strength functions for proton pair deposit and removal, respectively, for the nucleus ^{164}Dy. In each of them part A shows the uncorrelated strength function for HFB, and part B the correlated RPA. The underlying physics is very similar to that previously discussed, and we shall not go into details.

We now turn to discuss the nucleus ^{162}Dy. We shall not show all the transfer strength but just the neutron-pair transfer and only the correlated (RPA) results. They are shown in Figure 7, part A for pair removal and part B for pair addition. If we compare with the analogous cases in the ^{164}Dy nucleus we see that aside from small details, due to the change in the neutron number, most of the outstanding features are the same. A somewhat awkward feature is that for I = 16ħ, where the backbending occurs, the RPA breaks down. As we can see, this problem only affects the vicinity of the Yrast state and just for this I-value.

A quantitative comparison with the experimental[12] results is difficult, since we are not calculating cross sections. However, our calculations do confirm the experimental findings of some spreading of the transfer strength when going to high angular momentum.

We shall now concentrate on the behavior of the strength function in the region where the simple minded theories (HFB) predict a pairing collapse. For ^{164}Dy at I=16ħ, we have an energy gap for neutrons of 300 KeV; for I=24ħ it is zero. If we now look at Fig. 3B, we find the transfer strengths at these spin values rather similar. In the same way, the neutron-gap at I=24ħ for ^{162}Dy is 0.4 MeV and for ^{164}Dy, as mentioned, zero; if we compare the strength functions at low excitation energy for these nuclei at this spin value, i.e.

Fig. 3B and Fig. 7B, we again do not find qualitative differences. From these two examples, where we compare the transfer strength of two cases, one with a pairing gap of the size expected at high spins, the other with gap zero, we see that there is no signal for a pairing collapse. Notice that this is not the case if one looks at the corresponding Figures in the HFB approximation. It appears[21] as if, in the small amplitude limit, correlation built in by the RPA were enough, to some extent, to smear out the sharp phase transition from a superconductor to a normal conductor. It is important to notice that in our RPA approach we use as starting point HFB wave functions that do experience a sharp pairing collapse and nevertheless we do not get clear signals in the strength functions. The use of projected theories, that do not predict a sharp pairing collapse, as a starting point will, probably, wash out even more the shown results.

IV. Conclusions

We have performed realistic calculations of the strength functions for pair-transfer for the nucleic ^{164}Dy and ^{162}Dy, as a function of the angular momentum and the excitation energy. We find in all cases a large increase of the transfer strength to the excited states at high spins. It concentrates somewhat within the lowest 4 MeV of excitation energy, and it is rather spread out without any given structure. We do not find in the strength functions any indication of a sharp phase transition from a superconductor to a normal conductor.

Acknowledgments

We thank R.R. Chasman for a careful reading of the manuscript and Roy Bossingham for the help with several computational problems. One of the authors (J.L.E.) would like to thank the Nuclear Science Division, especially R.M. Diamond and F.S. Stephens, for the hospitality extended to him during his stay at the Lawrence Berkeley Laboratory.

References

1. A. Johnson, H. Ryde, and S.A. Hjorth, Nucl. Phys. **A179**, 753 (1972).
2. B.M. Nyko et al., Phys. Rev. Lett. **52**, 507 (1984).
3. C. Baktash et al., Phys. Rev. Lett. **54**, 978 (1985).
4. S.B. Patel et al., Phys. Rev. Lett. **57**, 62 (1986).
5. J.O. Newton et al., Phys. Rev. Lett. **46**, 1383 (1981).
6. J.C. Bacelar et al., Phys. Rev. Lett. **55**, 1858 (1985).
   J.E. Draper et al., Phys. Rev. Lett. **56**, 309 (1986).
7. B.R. Mottelson and J.G. Valatin, Phys. Rev. Lett. **5**, 511 (1960).
8. J.L. Egido and P. Ring, Nucl. Phys. **A388**, 19 (1982).
9. R.A. Broglia and M. Gallardo, Nucl. Phys. **A467**, 4896 (1985).
10. M.W. Guidry et al., Nucl. Phys. **A361**, 275 (1981).
11. A.O. Maquiavelli et al., Nucl. Phys. **A432**, 436 (1985).
    C.H. Dasso et al., Z. Phys. **A317**, 187 (1984).
12. M.W. Guidry et al., Phys. Lett. **163B**, 74 (1985).
    S. Juuinen et al. UTK preprint (1986) to be submitted to Phys. Lett.
13. K. Kumar and M. Baranger, Nucl. Phys. **110**, 529 (1968).
14. A. Bohr and B.R. Mottelson, Nuclear Structure, Vol. II, (Benjamin, New York, 1985).
15. K. Kumar, Nucl. Phys. **A231**, 189 (1974).
16. H.J. Mang, Phys. Rep. **18C**, 325 (1975).
17. R.S. Nikam, P. Ring, and L.F. Canto, T.V.M. Preprint, 1986.
18. J.L. Egido, H.J. Mang, and P. Ring, Nucl. Phys. **A339**, 390 (1980).
19. A.L. Goodman, Nucl. Phys. **A230**, 466 (1974).
20. P. Ring and P. Schuck, The nuclear many-body problem (Springer, Heidelberg, 1980).
21. R.A. Broglia et al., Phys. Lett. **166B**, 252 (1986).

Figure Captions

Fig. 1 - Schematic illustration of a pair-transfer at finite spin.

Fig. 2 - (a) HFB results for the nucleus ^{162}Dy as a function of the angular momentum. Upper part, the gap parameters in MeV (r.h.s. scale) and cranking velocity in MeV (l.h.s. scale). Lower part, different alignments, see text for definition. (b) Same as (a) for ^{164}Dy.

Fig. 3A - The strength function for neutron-pair addition for ^{164}Dy, as a function of the excitation energy for several values of the angular momentum, using the HFB approach.

Fig. 3B -Same as Fig. 3A using the RPA approach

Fig. 4A -Same as Fig. 3A for neutron-pair removal.

Fig. 4B -Same as Fig. 3B for neutron-pair removal.

Fig. 5A -Same as Fig. 3A for proton-pair addition.

Fig. 5B -Same as Fig. 3B for proton-pair addition.

Fig. 6A -Same as Fig. 3A for proton-pair removal.

Fig. 6B -Same as Fig. 3B for proton-pair removal.

Fig. 7A - The strength function for the nucleus ^{162}Dy in the RPA for neutron-pair removal.

Fig. 7B -Same as Fig. 7A for neutron-pair deposit.

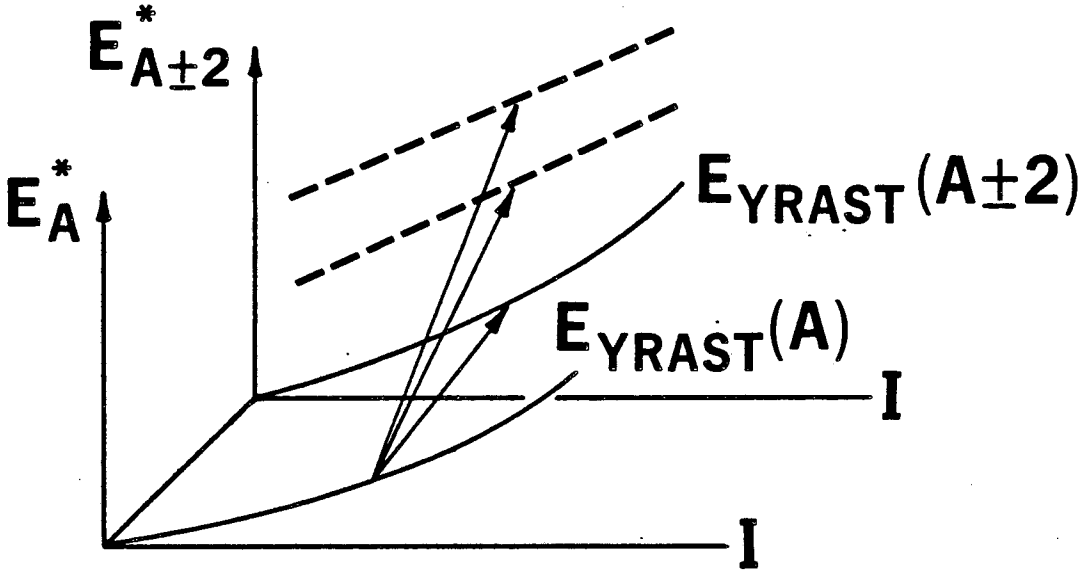

XBL 867-2752

Fig. 1

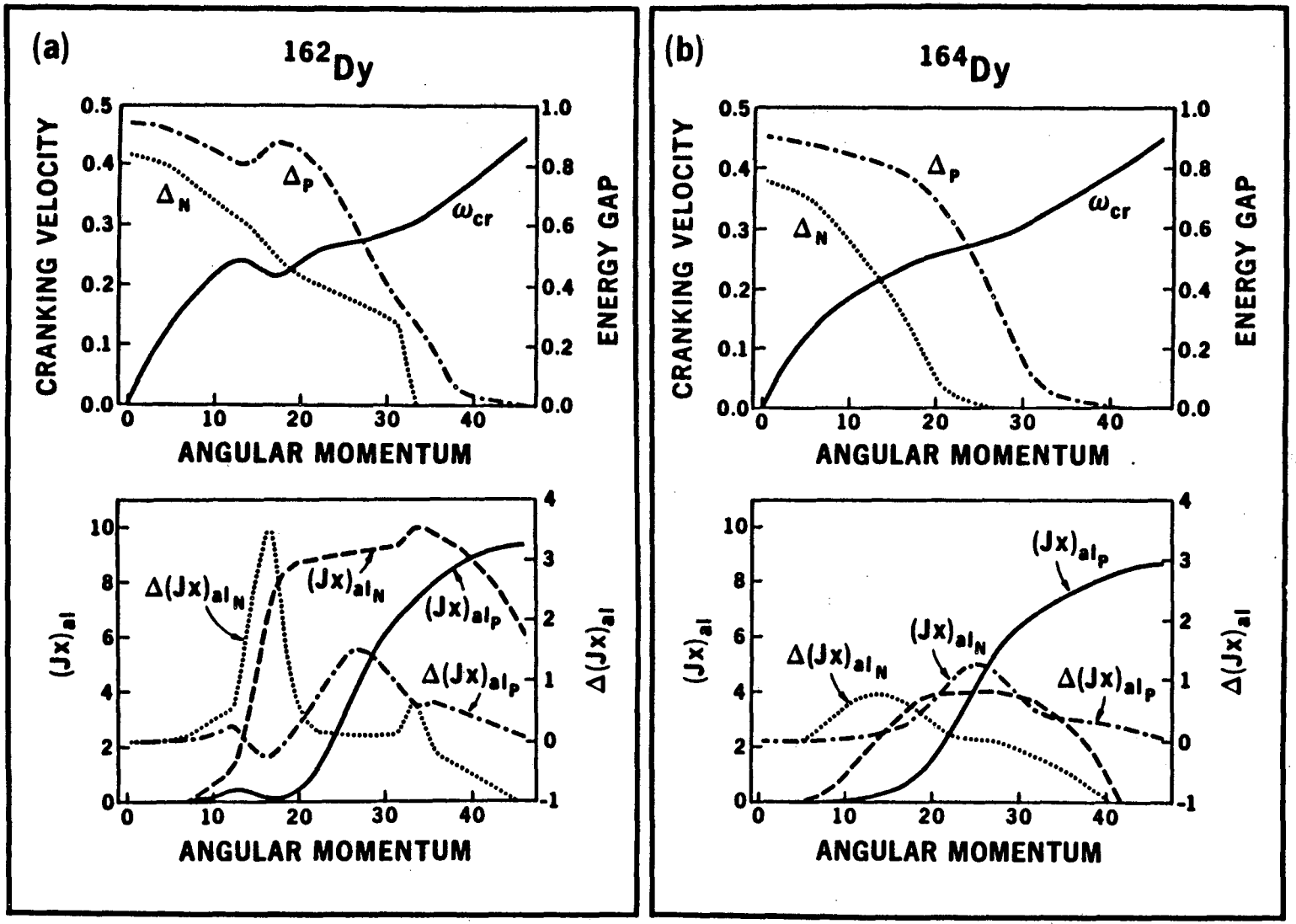

XBL 867-2751

Fig. 2

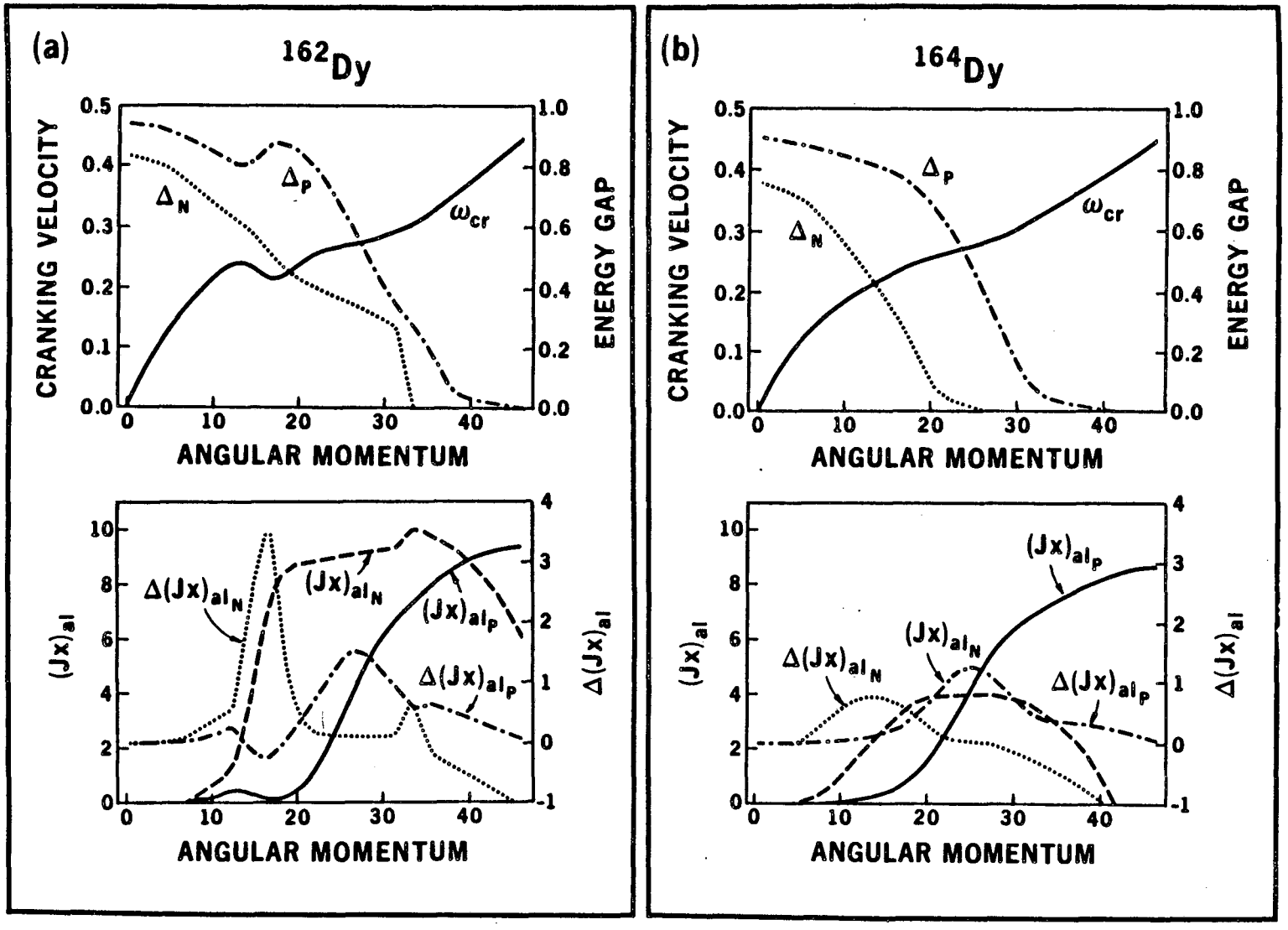

XBL 867-2751

Fig. 3

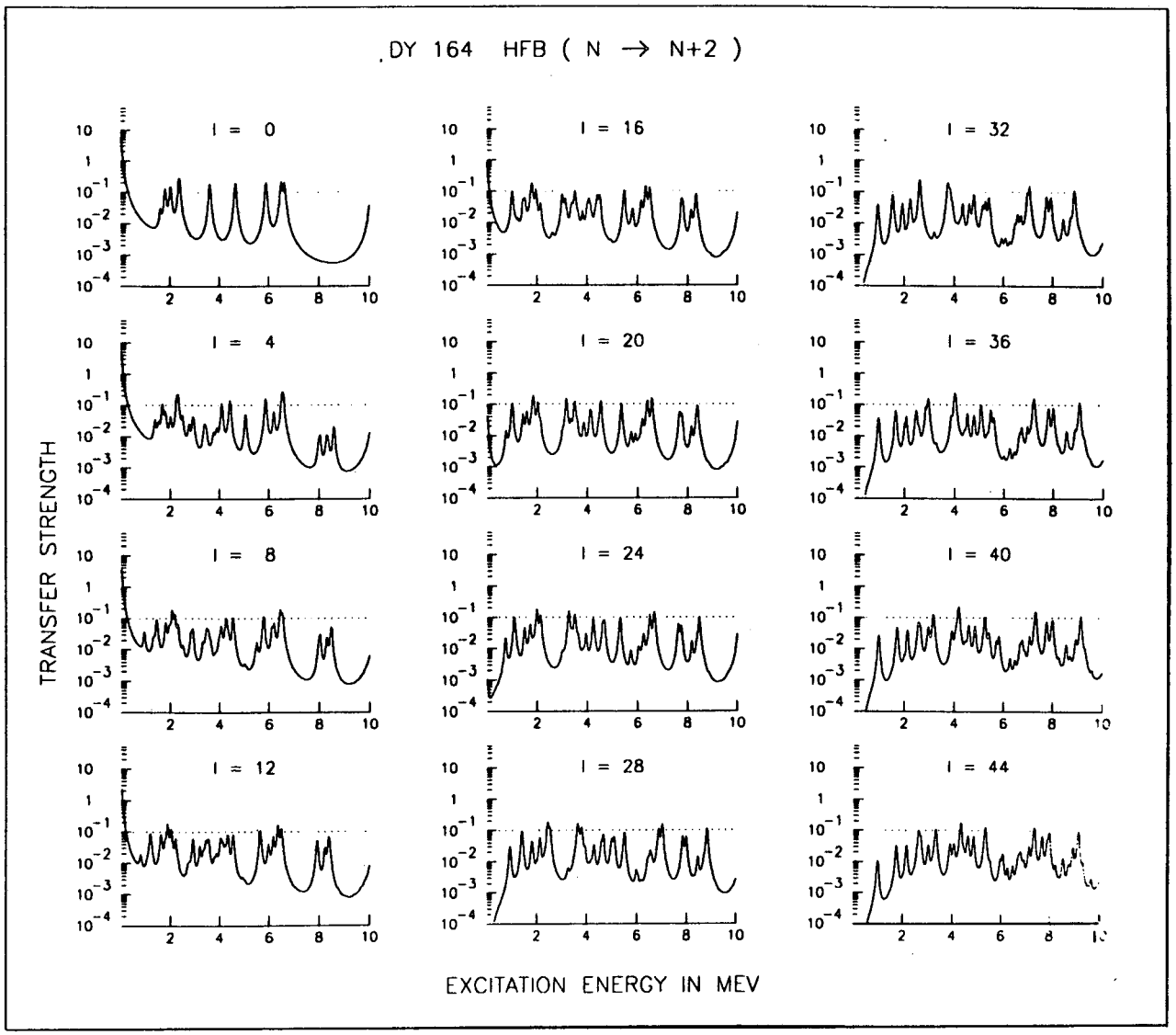

XBL 867-2717 A

Fig. 4

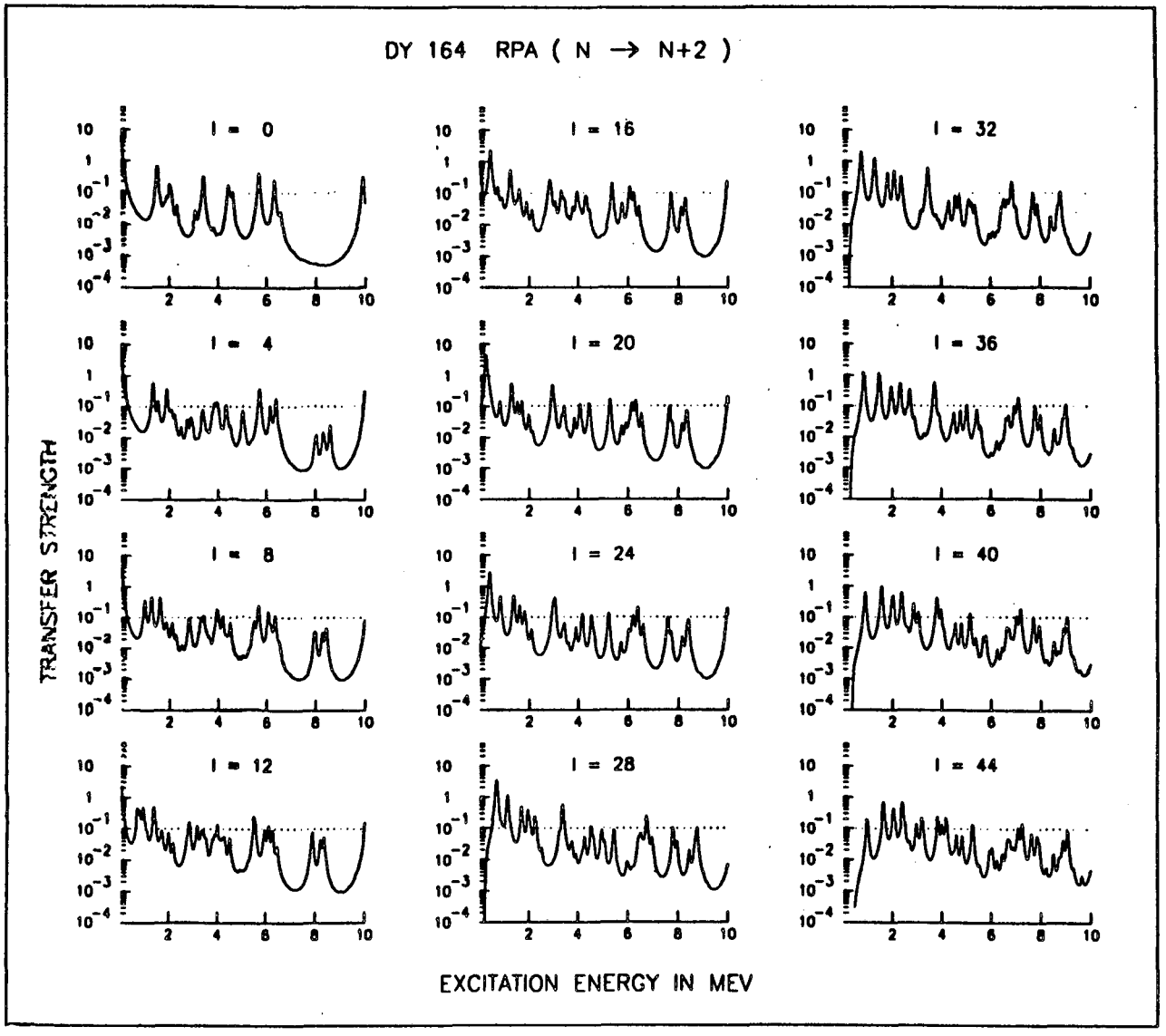

XBL 867-2717 B

Fig. 5

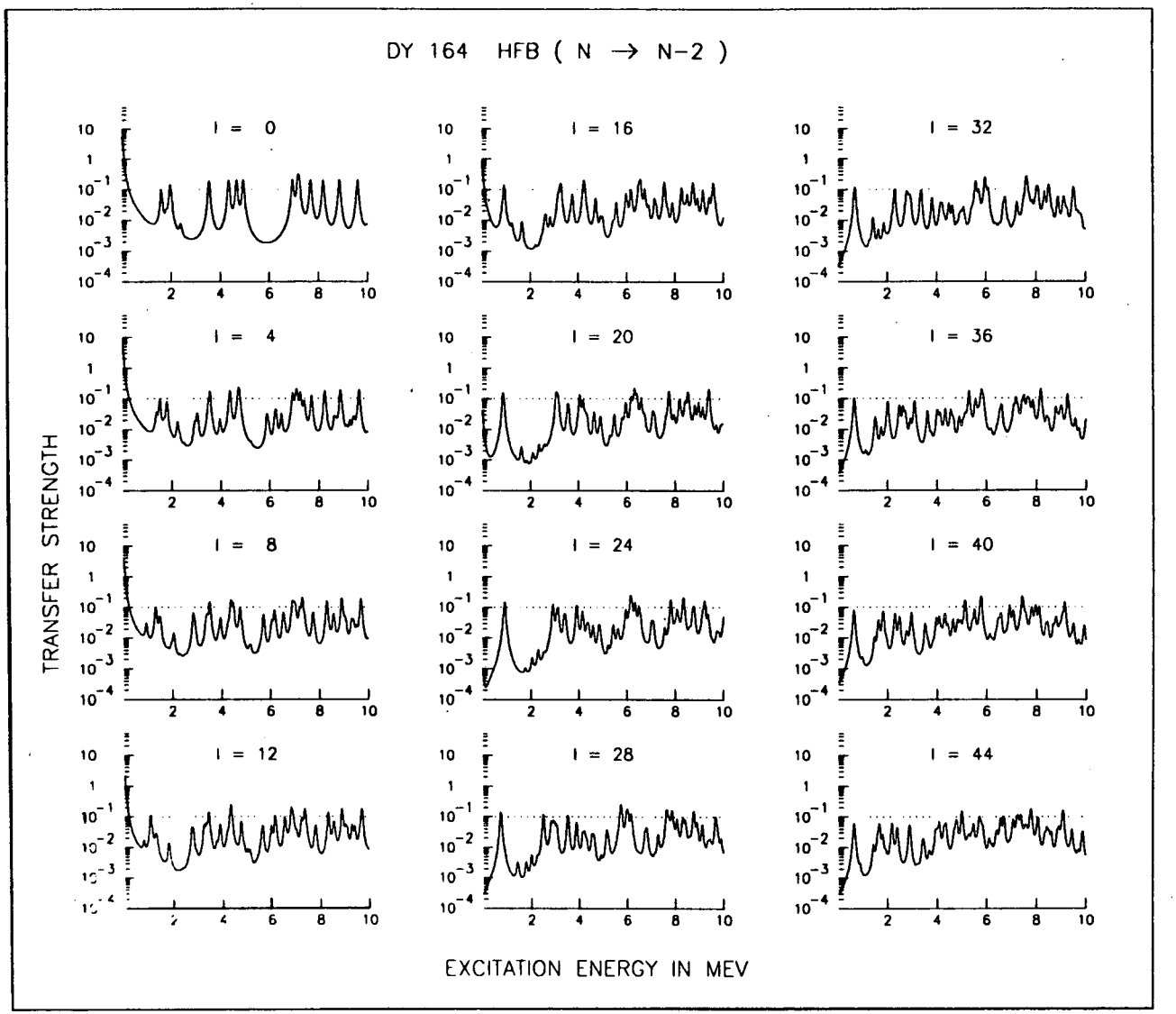

XBL 867-2718 A

Fig. 6

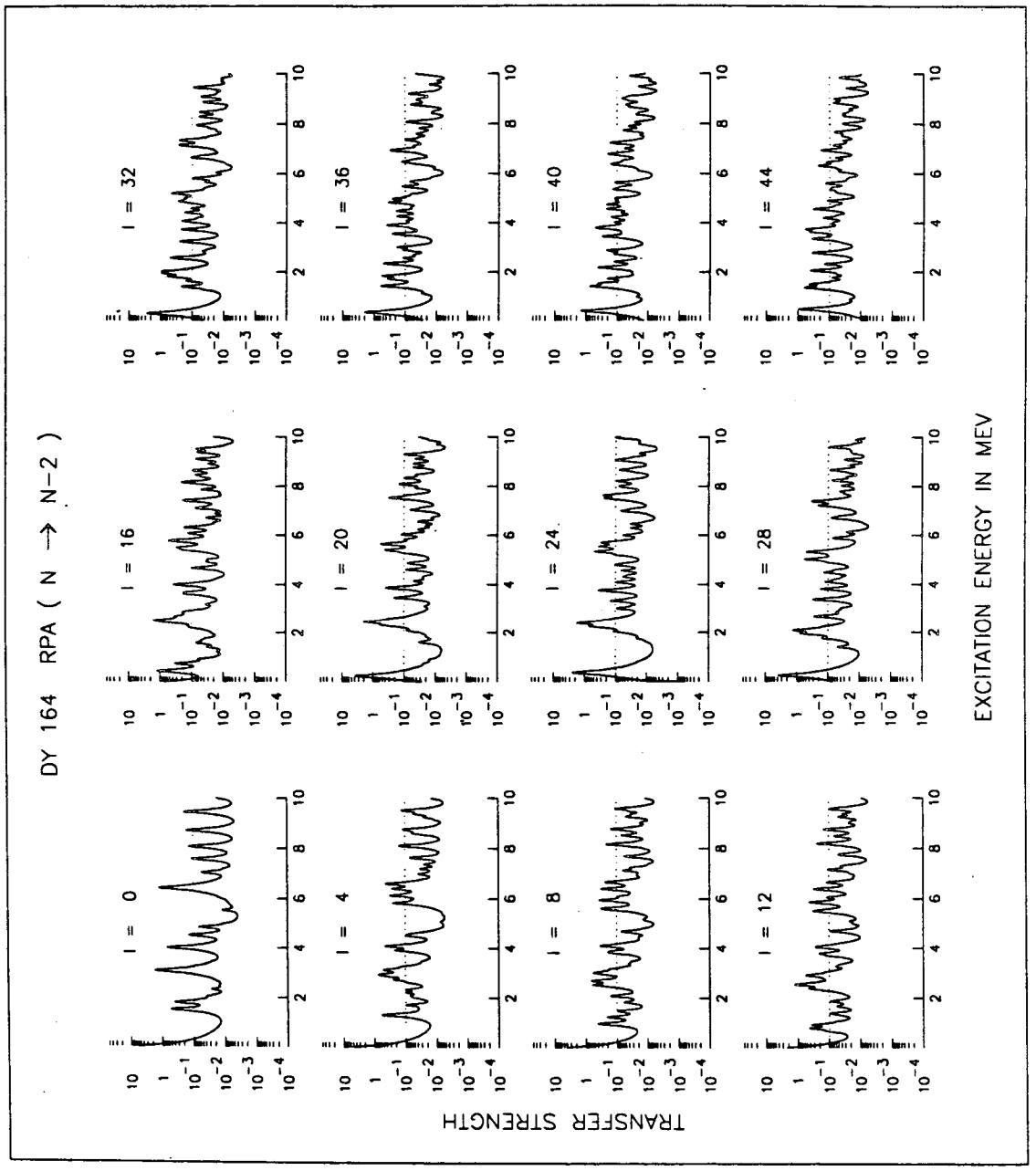

XBL 867-2718 B

Fig. 7

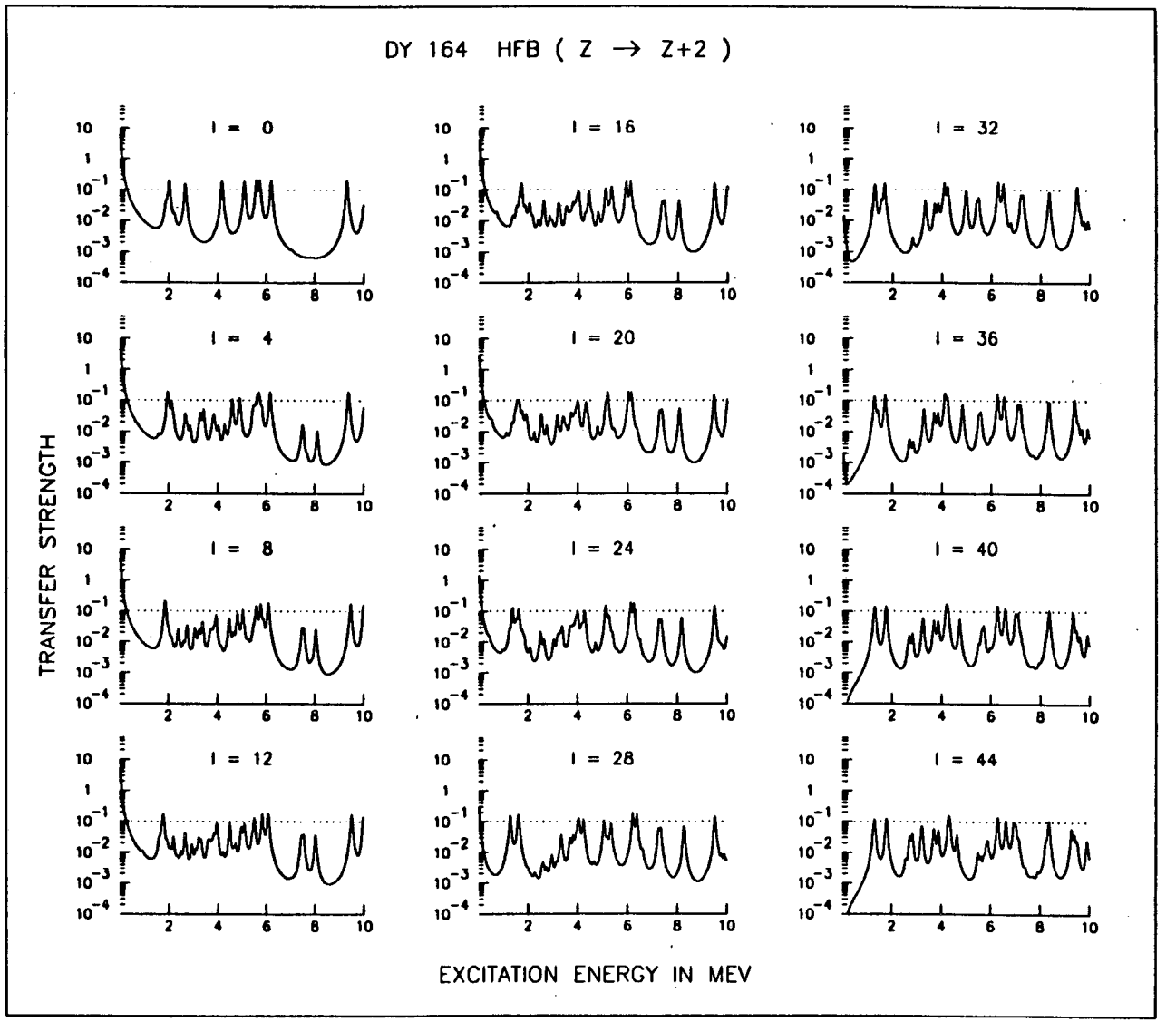

XBL 867-2719 A

Fig. 8

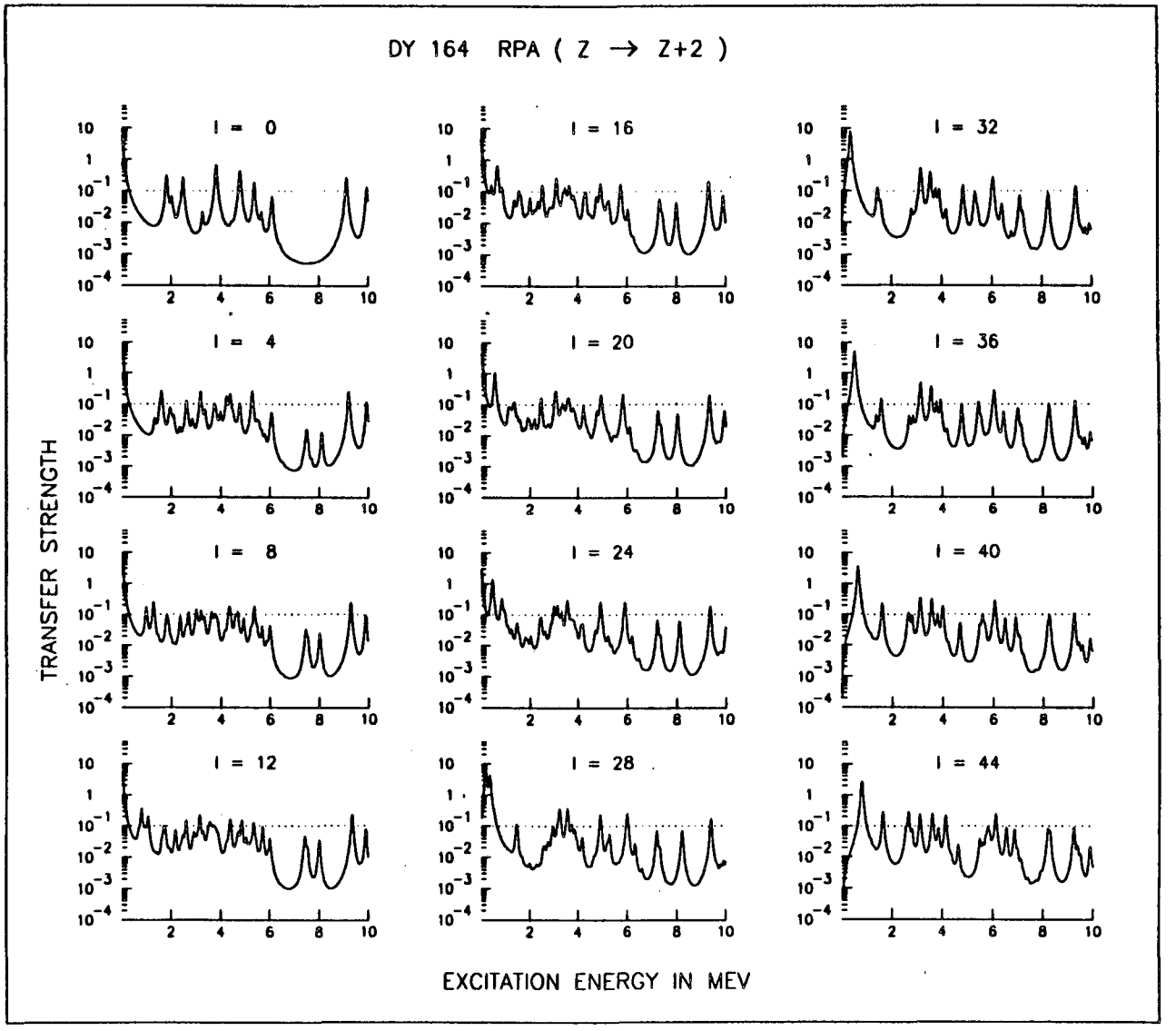

XBL 867-2719 B

Fig. 9

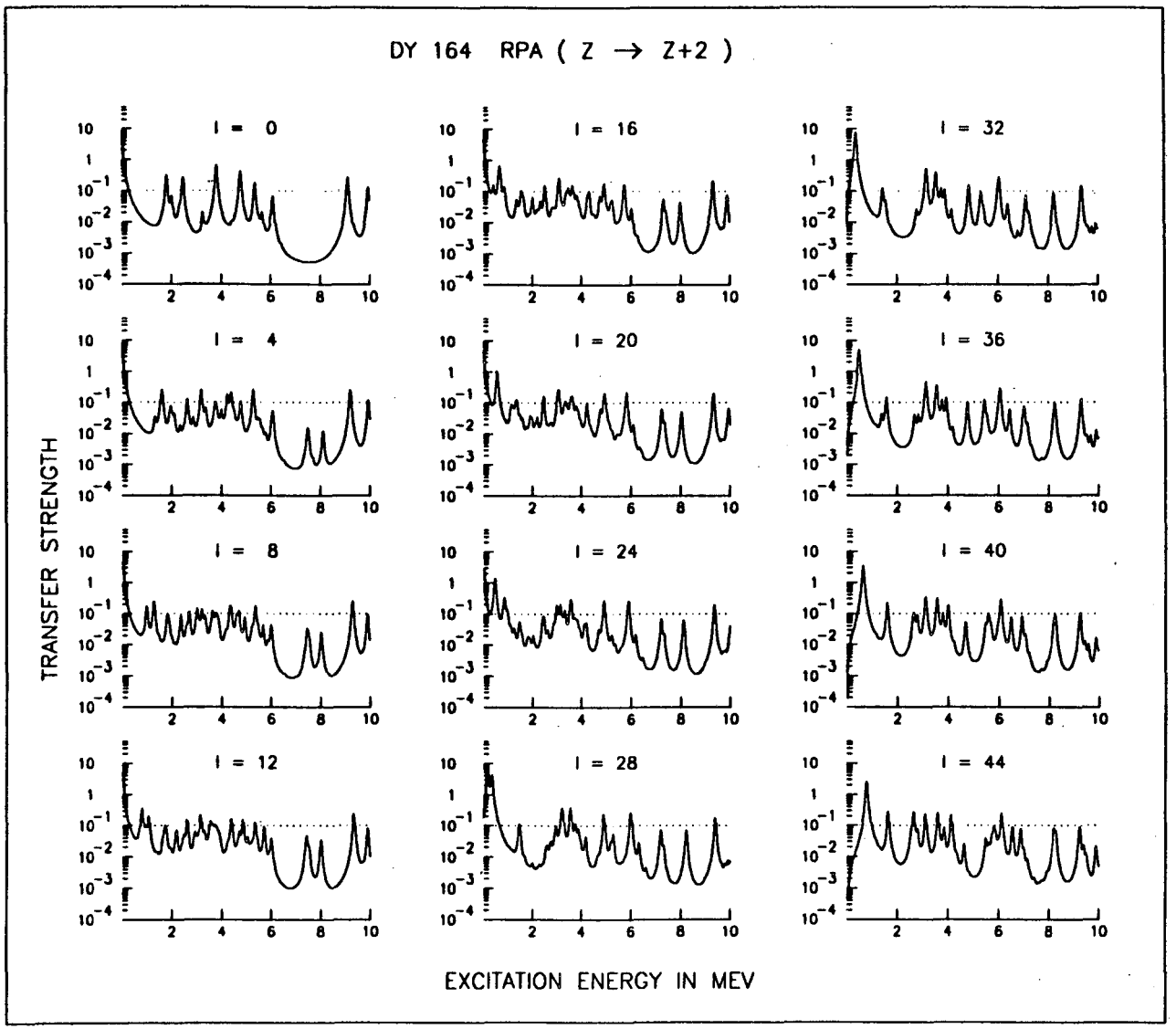

XBL 867-2719 B

Fig. 10

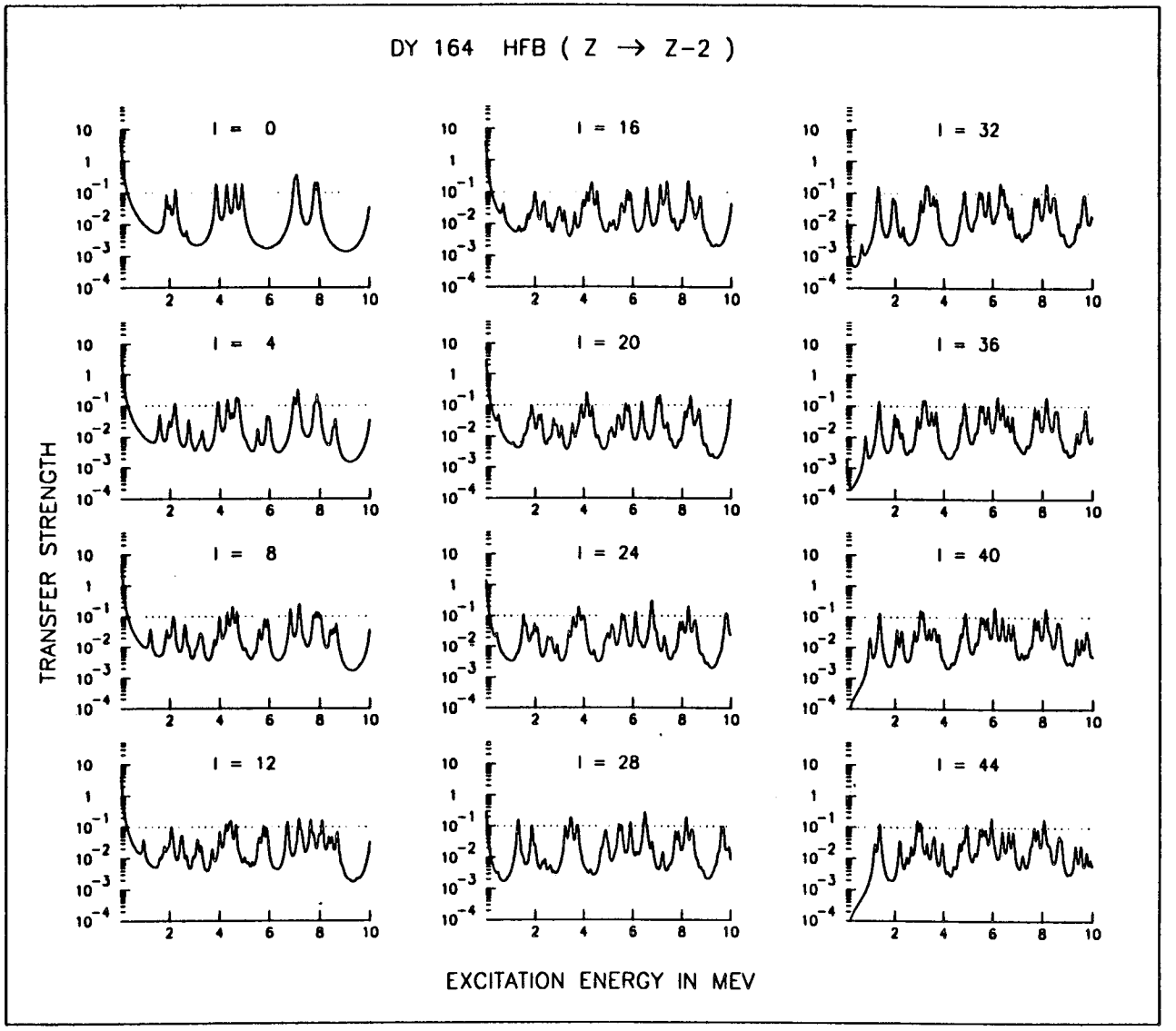

XBL 867-2720 A

Fig. 11

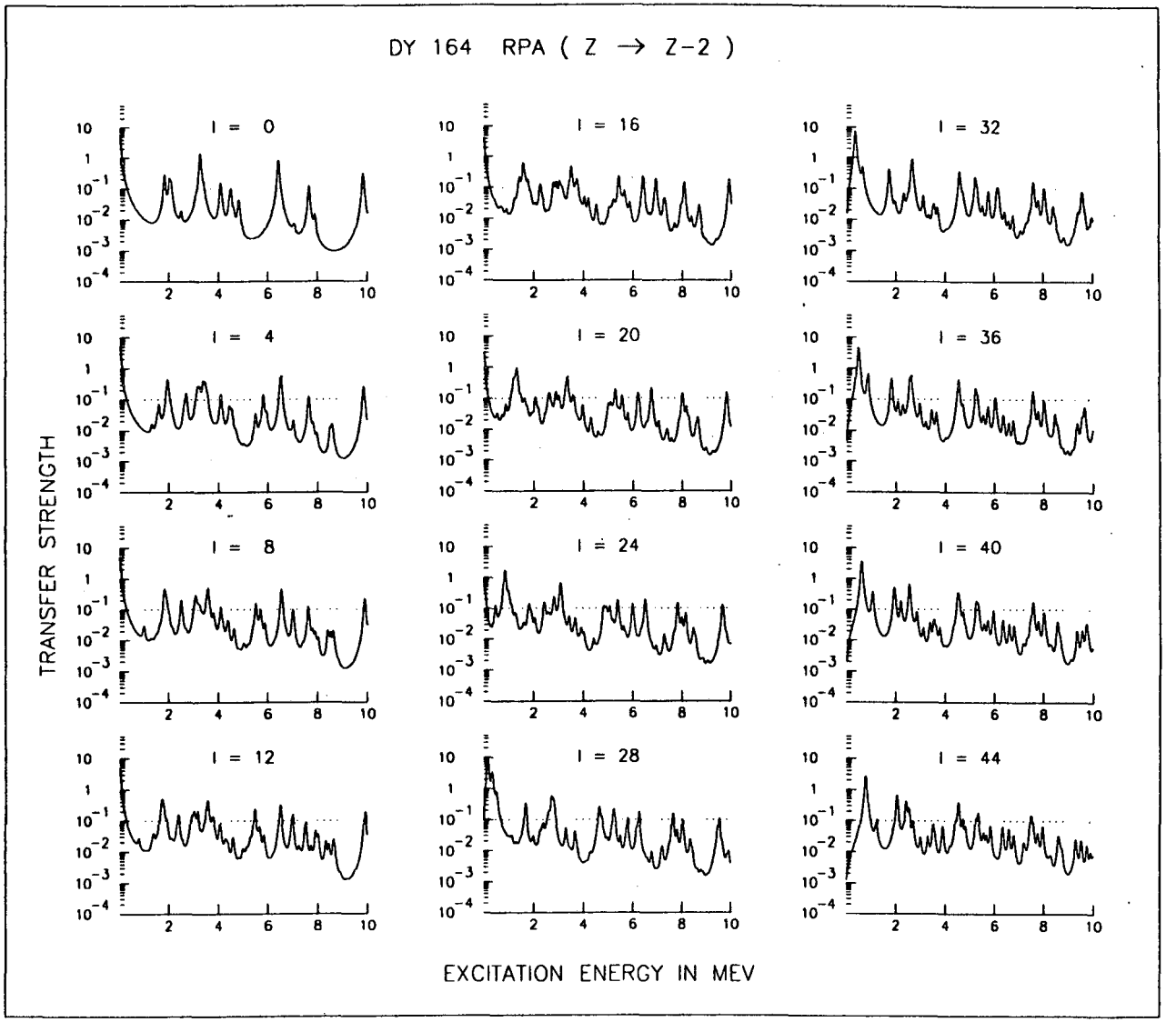

XBL 867-2720 B

Fig. 12

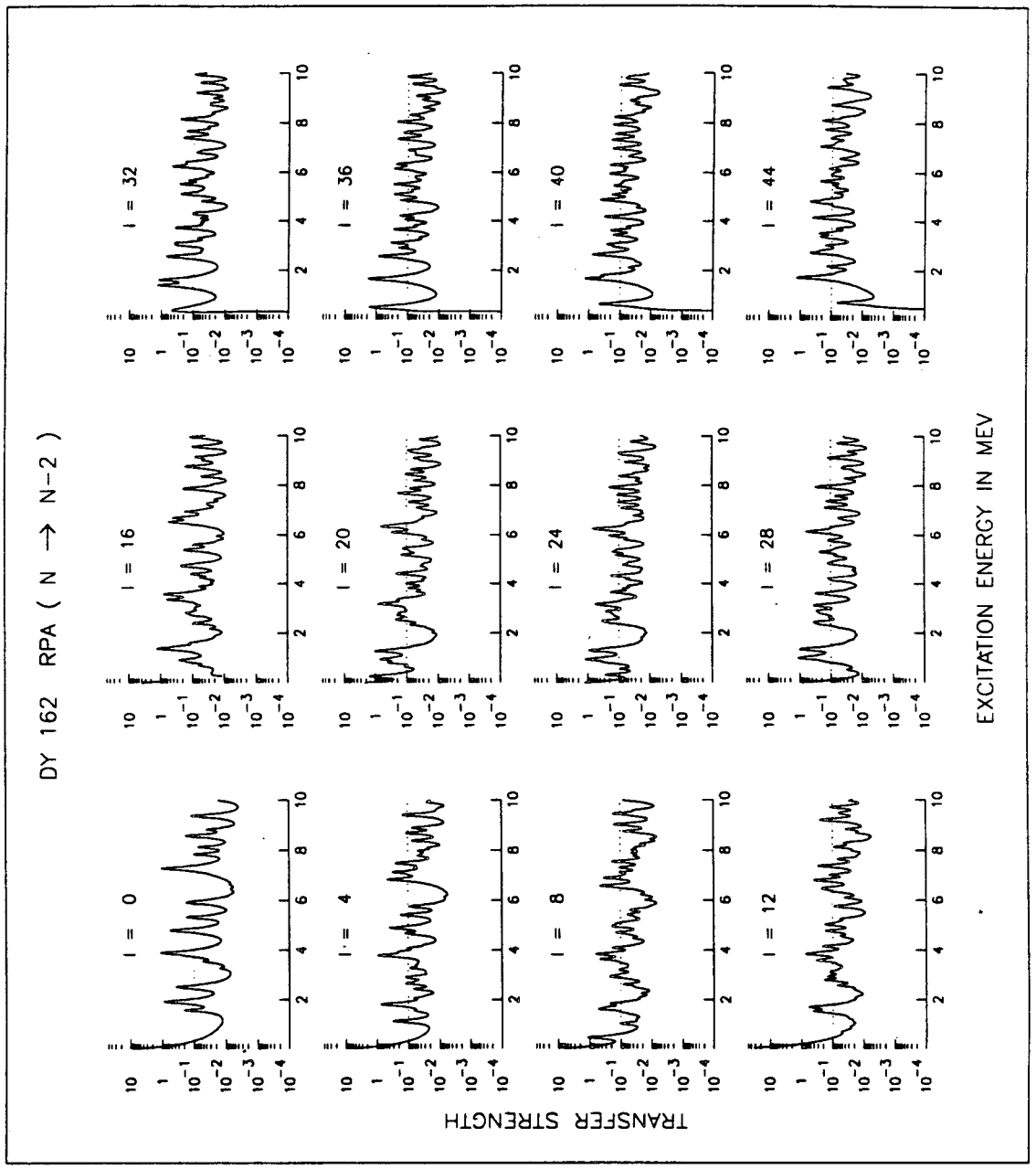

XBL 867-2716 A

Fig. 13

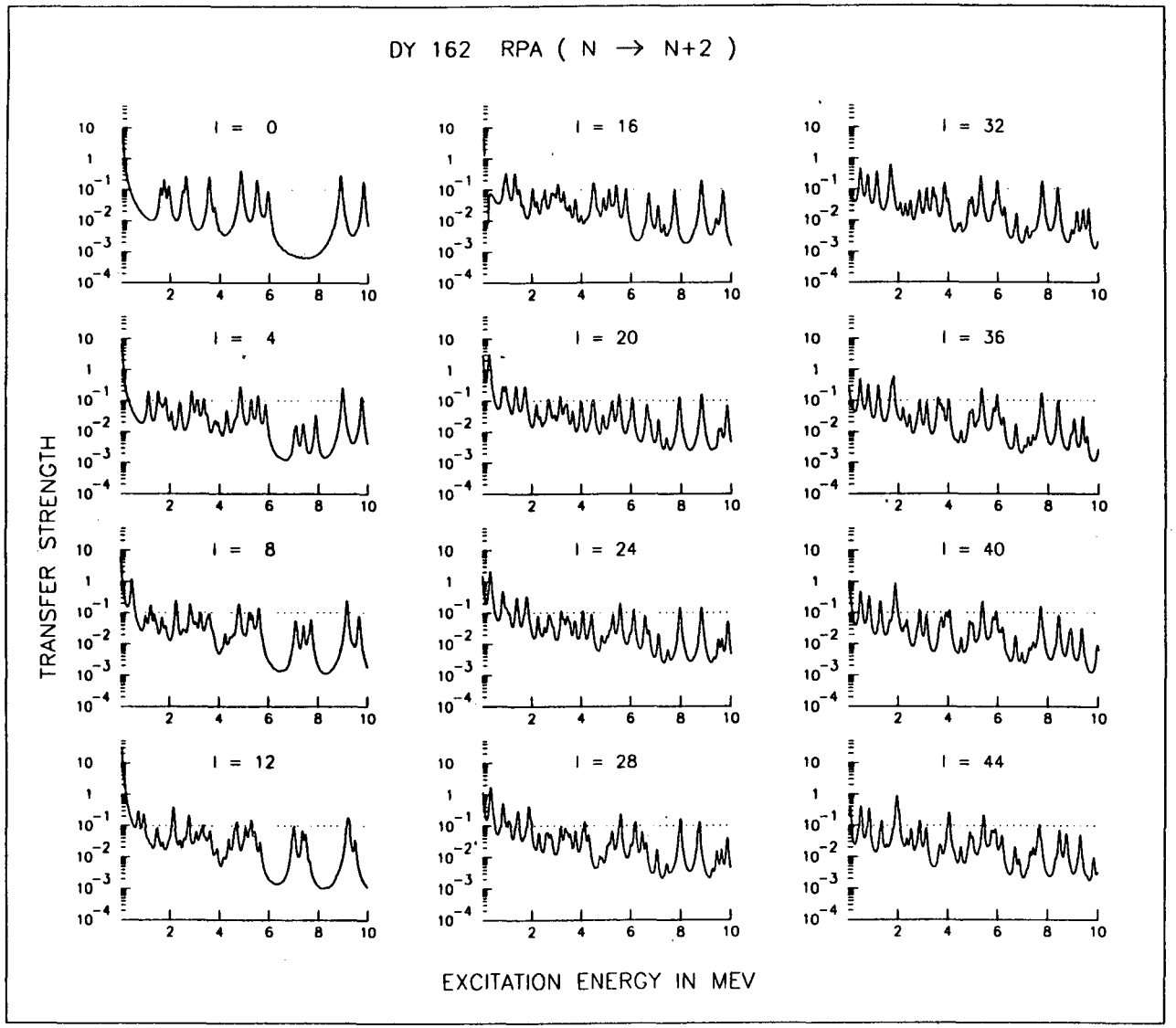

XBL 867-2716 B

Fig. 14

This report was done with support from the Department of Energy. Any conclusions or opinions expressed in this report represent solely those of the author(s) and not necessarily those of The Regents of the University of California, the Lawrence Berkeley Laboratory or the Department of Energy.

Reference to a company or product name does not imply approval or recommendation of the product by the University of California or the U.S. Department of Energy to the exclusion of others that may be suitable.

LAWRENCE BERKELEY LABORATORY
TECHNICAL INFORMATION DEPARTMENT
UNIVERSITY OF CALIFORNIA
BERKELEY, CALIFORNIA 94720